DOI:10.7598/cst2018.1466
ISSN:2278-3458

Chemical Science Transactions
2018, **7(2),** 163-180

RESEARCH ARTICLE

Adsorption and Corrosion Inhibition of *Cassia Angustifolia* (Senna) Fruit Extract on Mild Steel in Hydrochloric Acid Solution

A.S. FOUDA[*1], R. M. ABOU SHAHBA[2],
A. E. EL-SHENAWY[2] and TAGHREED J. A. SEYAM[3]

[1]Department of Chemistry, Faculty of Science, El-Mansoura University, El-Mansoura-35516, Egypt

[2]Department of Chemistry, Faculty of Science (Girls branch), Al-Azhar University, Cairo, Egypt

[3]Ministry of Education and Higher Education, Gaza, Palestine

asfouda@hotmail.com

Received 1 October 2017 / Accepted 26 October 2017

Abstract: *Cassia Angustifolia* (Senna) fruit extract as a corrosion inhibitor in 1 M HCl was investigated by using weight-loss (WL) method and electrochemical techniques. The effect of temperature on the corrosion inhibition of mild steel (MS) in the temperature range of 298-318 K was studied. Temperature studies indicated a decrease in inhibition efficiency (IE) with rise in temperature. The adsorption of Senna extract was found obey Langmuir adsorption isotherm. Polarization data revealed that this extract acts as mixed kind inhibitor. Surface analysis confirmed the formation of protective layer on MS surface. Results from various studies showed that Senna extract is an effective corrosion inhibitor for MS in 1 M HCl.

Keywords: *Cassia Angustifolia* extract, MS, Corrosion inhibition, HCl, Adsorption

Introduction

Iron and its alloys are one of the most consumed metals for constructional and industrial applications[1]. However, they are highly susceptible to corrosion, especially in acid media. Indeed, acid solutions are also widely used in industry for applications including acid pickling of steel and iron, ore production, chemical cleaning and processing and oil well acidification. Use of inhibitors is one of the most practical methods for protection against corrosion especially in acid solutions to prevent unexpected metal dissolution and acid consumption[2,3]. The efficiency of these inhibitors is related to the presence of polar functions with S, O or N atoms in the molecule, heterocyclic compounds and π-electrons[4-6]. Such compounds can adsorb onto the metal surface and block the active surface sites, thus reducing the corrosion rate. The polar function is usually regarded as the reaction center for the establishment of the adsorption process[7,8]. The known hazardous effects of most synthetic organic inhibitors and restrictive environmental regulations have made it necessary to search for cheaper, non-toxic and environmentally friendly natural

products as green corrosion inhibitors[9]. These natural organic compounds are either synthesized or extracted from aromatic herbs, spices and medicinal plants. Most of the natural products of plant origin are non-toxic, biodegradable and readily available in sufficient quantity in addition to meeting the structural considerations. Various plant parts: seeds, fruits, leave and flowers[10-20] were extracted and used as corrosion inhibitors. The results from these studies confirm that biomass extracts possess remarkable abilities to inhibit the corrosion reaction. *Cassia Angustifolia* (Senna) fruits extract belongs to the family Leguminosa, Senna has been widely acknowledged for medicinal purposes[21].

The aim of this work is to investigate the action of *Cassia Angustifolia* (Senna) fruits extract as corrosion inhibitor for MS in 1 M HCl solution using WL, potentiodynamic polarization (PP), electrochemical impedance spectroscopy (EIS) and electrochemical frequency modulation (EFM) techniques. Fourier transforms infrared spectroscopy (FT-IR), scanning electron microscope (SEM) and atomic force microscope (AFM) analyses were also used to confirm the mode of inhibition.

Figure 1. Photograph of *Cassia Angustifolia*

Experimental

The chemical composition of MS which was used in our investigation is given in weight %: C 0.068, Si 0.022, P 0.004, Mn 0.169, Ni 0.011, Cr 0.004, Mo 0.005, Cu 0.045, Ti 0.001, Co 0.005, Al 0.030, Fe balance.

Preparation of MS specimens

The specimens were mechanically cut into sizes with 2 × 2 × 2 cm dimensions and abraded by emery paper of different grades and finally polished with 2000 grade emery paper to obtain mirror-like finish. Each specimen was then degreased by washing with acetone and dried between two filter papers at room temperature.

Preparation of test solutions

The aggressive solution of 6 M HCl was prepared by dilution of analytical reagent grade 37% HCl with double distilled water and checked by standard Na_2CO_3 solution. All chemicals and reagents are Analar grade. The dose of test solution (1 M HCl) was prepared by dilution using double distilled water.

Preparation of Cassia Angustifolia (Senna) extract

The present investigation was carried out using the plant namely Senna. The samples were purchased from the local market and ground into a fine powder to give 200 g of powdered materials which extracted separately by soaking in 70% methanol (300 mL) for 48 h at room temperature. Then the methanolic extract of the sample was concentrated to nearly dryness under reduced pressure by using the rotary evaporator at 45 °C to achieve the crude methanolic extract which kept for further investigation[22]. The stock solution (1000 ppm) of Senna extract was used to prepare the desired dose by dilution with double distilled water. The dose range of Senna used was 50 to 300 ppm. Figure 1 illustrates the photograph of *Cassia Angustifolia*.

Measurement techniques

Weight loss method (chemical technique)

Seven parallel MS sheet of 2×2×2 cm were abraded with emery paper then initially weighed using an electronic balance. After that the specimens were suspended with the help of glass hooks in 100 mL beaker containing 1 M of acid in the presence and absence of various doses (50-300) ppm of Senna as corrosion inhibitor and the temperature between 298 and 318 K for an immersion period of 3 hours and the experiment was performed in a thermostatic water bath. After that they were dried and reweighed. The average value of the weight loss was noted. For each experiment, a freshly prepared solution was used, and the solution temperature was thermostatically controlled at a desired value. The (θ) and (IE %) was determined by using the following Eq.[23]:

$$\% \text{ IE} = \theta \times 100 = [1 - (\Delta W_{inh}/\Delta W_{free})] \times 100 \quad (1)$$

Where ΔW_{free} and ΔW_{inh} is the weight losses of metal per unit area in the absence and presence of plant extract, respectively at given time period and temperature.

Electrochemical techniques

Electrochemical measurements, including PP, EIS and EFM techniques were used. The electrochemical studies were made using a Gamry three-electrode cell assembly at room temperature. The MS of 1 cm^2 was the working electrode, platinum electrode was used as an auxiliary electrode, and saturated calomel electrode was used as reference electrode. The working electrode was abraded with different grades of emery papers, washed with double distilled water and degreased with acetone then dried between two filter papers. All the experiments were performed for metal specimens in 100 mL of 1 M HCl with and without various doses of the plant extract at room temperature. All electrochemical measurements were performed using Gamry Instrument (PCI4/750) Potentiostat/ Galvanostat/ZRA. This includes a Gamry framework system based on the ESA 400. Gamry applications include DC105 software for potentiodynamic polarization, EIS 300 software for electrochemical impedance spectroscopy, and EFM 140 software for electrochemical frequency modulation measurements via computer for collecting data.

Potentiodynamic polarization (PP) tests

The Tafel curves were obtained potentiodynamically between - 0.1 to 0.2 V with the scan rate of 1 mVs^{-1}. According to the Stern-Geary equation, the steps of the linear polarization plot are substituted to get corrosion current[24]. The IE % and (θ) were calculated using Eq. 2:

$$\% \text{ IE} = \theta \times 100 = [1 - (i_{inh} / i_{free})] \times 100 \quad (2)$$

Where i_{free} and i_{inh} are the corrosion current densities of uninhibited and inhibited solution, respectively.

Electrochemical impedance spectroscopy (EIS) tests

EIS was conducted with an open circuit potential in the frequency range of (1 Hz to 100 kHz) at an amplitude of 10 mV. Electrochemical parameters such as R_{ct} and C_{dl} values were obtained and the IE % was estimated from the charge transfer resistance (R_{ct}) obtained from the real (Z') *vs.* imaginary (Z") plot. The impedance diagrams were plotted in the Nyquist and Bode representation. The IE% and (θ) were obtained from the EIS measurements using Eq. 3:

$$\% \text{ IE} = \theta \times 100 = [1 - (R^{o}_{ct} / R_{ct})] \times 100 \quad (3)$$

Where R^{o}_{ct} and R_{ct} are the charge transfer resistance in the absence and presence of the used extract inhibitor, respectively.

Electrochemical frequency modulation (EFM) tests

EFM is used as a new technique for corrosion rate measurements[25]. EFM measurements were performed by applying potential perturbation signal with amplitude of 10 mV with two sine waves of 2 and 5 Hz. The intermodulation spectra contain current responses assigned for harmonical and intermodulation current peaks. The larger peaks were used to calculate the corrosion current density (i_{corr}), the Tafel slopes (βa and βc) and the causality factors CF2 and CF3[26].

Surface morphology

Scanning electron microscope (SEM) analysis

Surface examination of MS specimens in the absence and presence of the optimum dose (300 ppm) of the *Cassia Angustifolia* extract immersed for 24 h at room temperature was studied using (JEOL JSM-5500, JAPAN) model.

Atomic force microscopy (AFM) analysis

Atomic force microscopy is a useful tool to access the details of corrosion process at the molecular level. To capture the surface images, prepared MS samples were immersed in 1 M HCl without and with *Cassia Angustifolia* extract. After 24 h the specimens were taken out, cleaned with distilled water and dried. Thus obtained samples were analyzed by using a Pico SPM2100 AFM device operating in contact mode in air at Nanotechnology Laboratory, Faculty of Engineering, Mansoura University, Egypt.

Fourier transforms infrared spectroscopy (FT-IR) analysis

The coins MS were accumulated in 100 mL of 1 M HCl in the nonexistence and existence of 300 ppm of Senna extract at room temperature. After 4 h, the coins were removed and dried by air. Then, the MS surface coating on the coins has carefully scratched and the gotten coins utilized to the FT-IR spectra test. IR Affinity (Perkin-Elmer) spectrophotometer was used for recording the FT-IR spectra to define the composition of the corrosion product obtained on the surface of MS.

Results and Discussion

Weight loss (WL) measurements

WL- time curves of MS in 1 M HCl was determined in the absence and presence of different doses of Senna and is shown in Figure 2. The obtained corrosion parameters are depicted in Table 1. It is clear from the Table that the IE% increases with dose of the Senna extract and decreases with increasing temperature. The decrease in corrosion rate (CR) with increase in dose of Senna is due to the fact that the (θ) of metal increases by the adsorption of inhibitor molecules[27]. The increase in CR with increase in temperature may be probably due to increased rate of desorption of inhibitor molecules of Senna from the MS surface at higher temperatures[28].

Potentiodynamic polarization (PP) measurements

PP measurements were carried out to study the effect of Senna extract on the anodic and cathodic reactions occurring in the system. From Table 2, it can be seen that i_{corr} values are decreasing with increasing inhibitor dose, which evidently shows corrosion inhibition. From Figure 3, it is evident that *Cassia Angustifolia* extract retard both cathodic and anodic processes, which is also supported by the data given in Table 2**.** Both β_a and β_c values have changed, and it can be seen that there is no regular displacement pattern in the E_{corr} values which shows that both the inhibitor acts as mixed type. According to Ferreira and others[29], if the displacement in corrosion potential is more than 85 mV with respect to the corrosion potential of the blank, the inhibitor can be seen as a cathodic or anodic type. In the present study the maximum displacement was 23 mV, indicating that the studied inhibitor is a mixed type inhibitor.

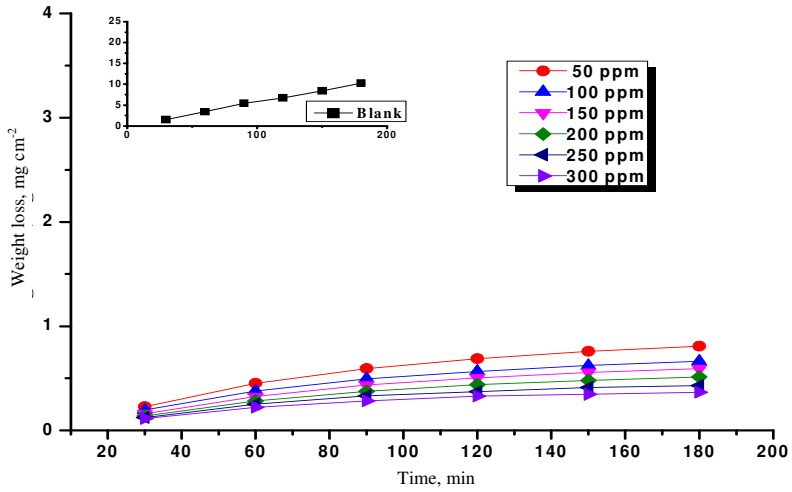

Figure 2. Weight loss *vs.* time curves for the corrosion of MS in 1 M HCl in the absence and presence of different doses of Senna extract at 25 ^{o}C

Table 1. Data of weight loss measurements for MS in 1 M HCl solution in the absence and presence of different doses of Senna extract at 25-45 ^{o}C

Conc., ppm	Temp., ^{o}C	C.R., mg cm^{-2}min^{-1}	Θ	%IE
	25	0.0057	0.898	89.8
	30	0.0088	0.881	88.1
50	35	0.0148	0.865	86.5
	40	0.0230	0.838	83.8
	45	0.0305	0.814	81.4
	25	0.0047	0.916	91.6
	30	0.0081	0.890	89
100	35	0.0135	0.878	87.7
	40	0.0204	0.857	85.7
	45	0.0277	0.831	83.1
	25	0.0042	0.925	92.5
	30	0.0073	0.901	90.1
150	35	0.0119	0.891	89.1
	40	0.0185	0.870	87
	45	0.0266	0.838	83.8
	25	0.0037	0.935	93.5
	30	0.0064	0.913	91.3
200	35	0.0103	0.906	90.6
	40	0.0172	0.879	87.9
	45	0.0241	0.853	85.3
	25	0.0031	0.945	94.5
	30	0.0057	0.922	92.2
250	35	0.0092	0.916	91.6
	40	0.0151	0.894	89.4
	45	0.0212	0.871	87.1
	25	0.0027	0.951	95.1
	30	0.0046	0.938	93.8
300	35	0.0078	0.929	92.9
	40	0.0121	0.915	91.5
	45	0.0174	0.894	89.4

Table 2. Potentiodynamic polarization data of MS in 1 M HCl in the absence and presence of different doses of Senna extract at 25 °C

[inh] ppm	- E_{corr}, mV vs SCE	i_{corr}, μA cm^{-2}	β_c mV dec^{-1}	β_a mV dec^{-1}	C.R, mpy	Θ	% IE
Blank	528	1250	132	94	445	-	-
50	520	118	105	65	55	0.906	90.6
100	518	92	95	68	48	0.926	92.6
150	522	88	98	71	40	0.930	93.0
200	505	76	104	73	32	0.939	93.9
250	510	70	110	67	26	0.944	94.4
300	515	61	103	78	22	0.951	95.1

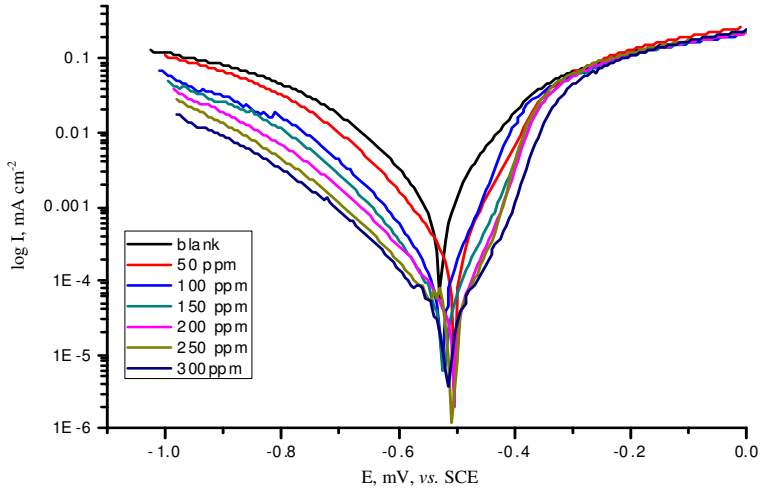

Figure 3. Potentiodynamic polarization curves for the corrosion of MS in 1 M HCl in the absence and presence of various doses of Senna extract at 25 °C

Electrochemical impedance studies (EIS) measurements

EIS is a well-established and powerful tool in corrosion studies. The electrochemical process taking place at the open circuit potential was studied by EIS in order to obtain an understanding of the mechanistic, electrode kinetics, surface properties of MS corrosion in the presence of an inhibitor[30]. The Nyquist plots Figure 4a contain a semicircle; the diameter of this is increased by increasing the inhibitor dose. This indicates that inhibition efficiency is directly proportional to the dose of inhibitor. The shape of the capacitive loops shows that the corrosion process was mainly charge transfer controlled[31]. The increase in charge transfer resistance (R_{ct}) with inhibitor dose indicates considerable surface coverage by the inhibitor and strong bonding to the surface. The Nyquist plots are analyzed in terms of the equivalent circuit Figure 5, which is generally used to describe EIS data. The R_{ct} values increased and double layer capacitance (C_{dl}) values decreased with increase in extract dose, which is a probably due to the decrease in the local dielectric constant or an increase in the thickness of the electrical double layer. This suggests that the inhibitor strongly adsorbed on the surface of MS[32]. The increase in the R_{ct} values and decrease in the C_{dl} values result in an increase in the inhibition efficiency. The results were observed for MS in the 1 M HCl medium in the absence and presence of various doses of Senna extract. As the Nyquist plot obtained for the present of the inhibitor are exhibits a loop, such behavior is characteristic for solid

electrodes and is often attributed to a frequency dispersion resulting from the surface irregularity. The C_{dl} values were obtained from Eq. 4:

$$C_{dl} = 1 / 2\pi R_{ct} f_{max} \quad (4)$$

Where f_{max} represents the frequency at which imaginary value reaches a maximum on the Nyquist plots. In the Bode plots Figure 4b, the high frequency limits corresponds to the solution resistance R_S (Ω), while the lower frequency limits corresponds to (R_{ct} + R_s). The low frequency shows the kinetic response of the charge transfer reaction[33]. The corrosion parameters from impedance measurements are given in Table 3. The obtained results show that the value of R_{ct} increases with increasing the dose of Senna, which leads to an increase in %IE and values of double layer capacitance (C_{dl}) decrease in the presence of the inhibitor. The decrease in C_{dl} results from a decrease in local dielectric constant and/or an increase in the thickness of the double layer. Thus, it is reasonable to reduce that inhibitor extract function by adsorption at the metal- acid interface[34]. It is clear that there is a good agreement between the two different electrochemical techniques, due to that the same trend of inhibition of Senna extract.

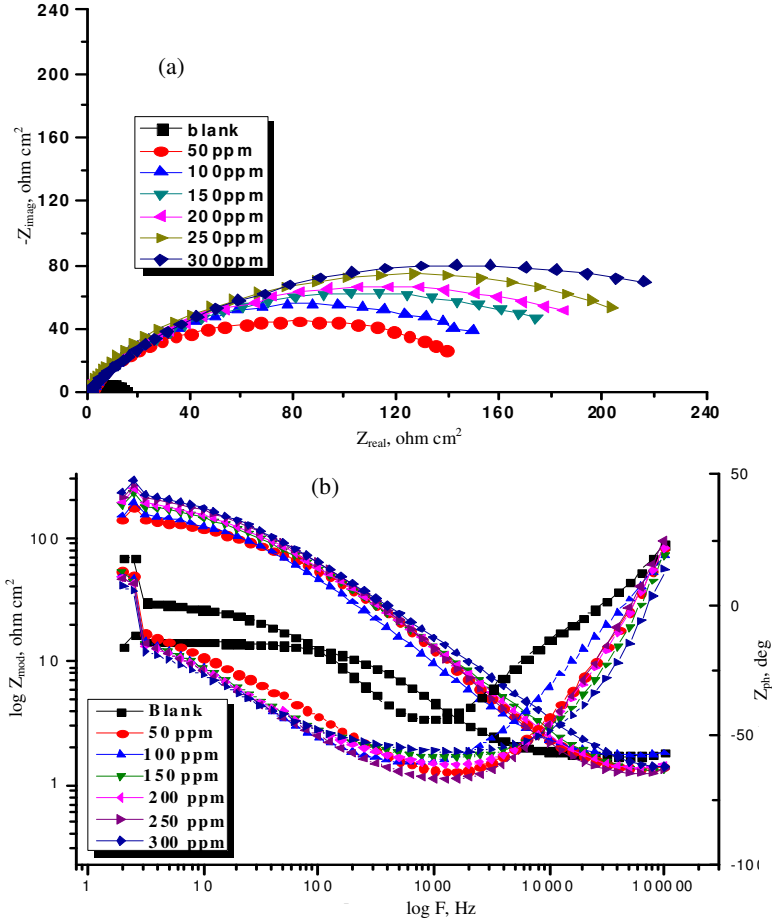

Figure 4. The Nyquist (a) and Bode (b) plots for the corrosion of MS in 1 M HCl in the absence and presence of different doses of Senna extract at 25 ^{o}C

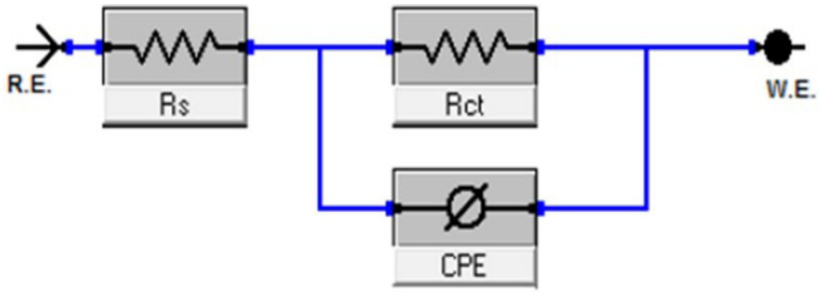

Figure 5. Equivalent circuit used to model impedance data for MS in 1 M HCl solutions.

Table 3. EIS parameters for the corrosion of MS in 1 M HCl in the absence and presence of different doses of Senna extract at 25° C

[inh.] ppm	R_{ct}, Ω cm^2	C_{dl}, µFcm^{-2}	Θ	%IE
Blank	12.3	47	-	-
50	133.2	37.1	0.907	90.7
100	157.5	33.58	0.921	92.1
150	180.6	30.20	0.931	93.1
200	192.4	28.74	0.936	93.6
250	205.5	27.29	0.940	94.0
300	241.2	23.2	0.949	94.9

Electrochemical frequency modulation (EFM) measurements

The current-frequency spectral chart obtained from EFM measurements in the absence and presence of different doses of Senna extract is shown in Figure 6. The spectra were analyzed to calculate i_{corr}, β_a, β_c and the causality factors (CF-2 and CF-3) which are listed in Table 4. It can be seen from the Table that i_{corr} decreases with increase in Senna extract dose and the IE increases by increasing the extract dose. The change in magnitudes of β_a and β_c values was also small indicating that the presence of extract does not change the corrosion mechanism. The causality factors, CF-2 and CF-3, obtained were close to theoretical values of 2 and 3 respectively, showing that the obtained data are verified and good quality[35].

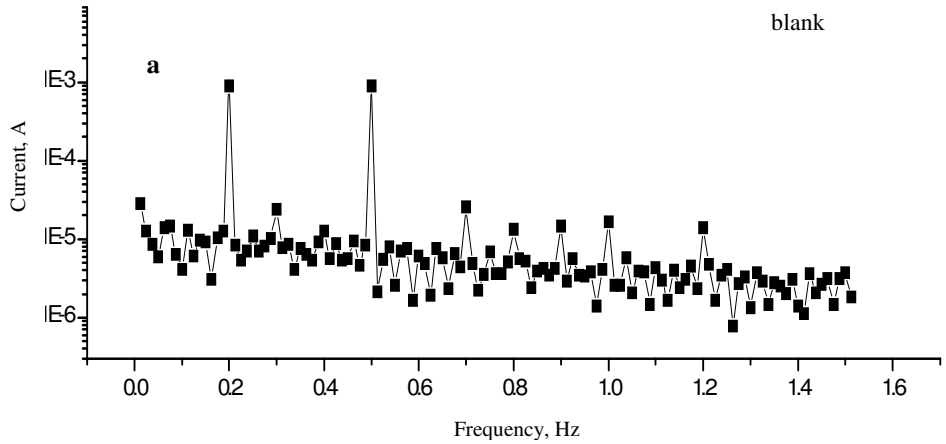

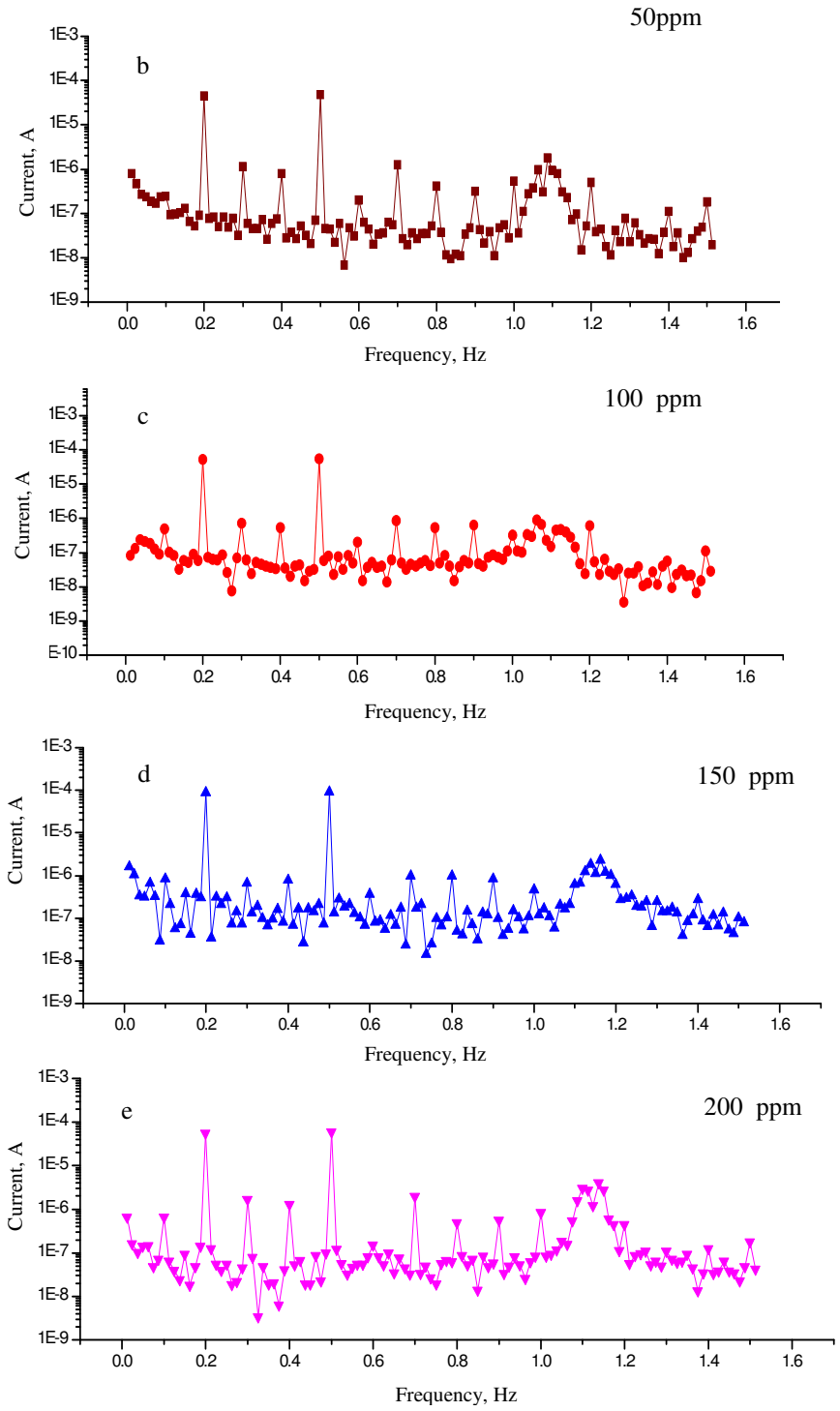
50ppm
b
Current, A
1E-3
1E-4
1E-5
1E-6
1E-7
1E-8
1E-9
0.0
0.2
0.4
0.6
0.8
1.0
1.2
1.4
1.6
Frequency, Hz
100 ppm
c
Current, A
1E-3
1E-4
1E-5
1E-6
1E-7
1E-8
1E-9
E-10
0.0
0.2
0.4
0.6
0.8
1.0
1.2
1.4
1.6
Frequency, Hz
150 ppm
d
Current, A
1E-3
1E-4
1E-5
1E-6
1E-7
1E-8
1E-9
0.0
0.2
0.4
0.6
0.8
1.0
1.2
1.4
1.6
Frequency, Hz
200 ppm
e
Current, A
1E-3
1E-4
1E-5
1E-6
1E-7
1E-8
1E-9
0.0
0.2
0.4
0.6
0.8
1.0
1.2
1.4
1.6
Frequency, Hz

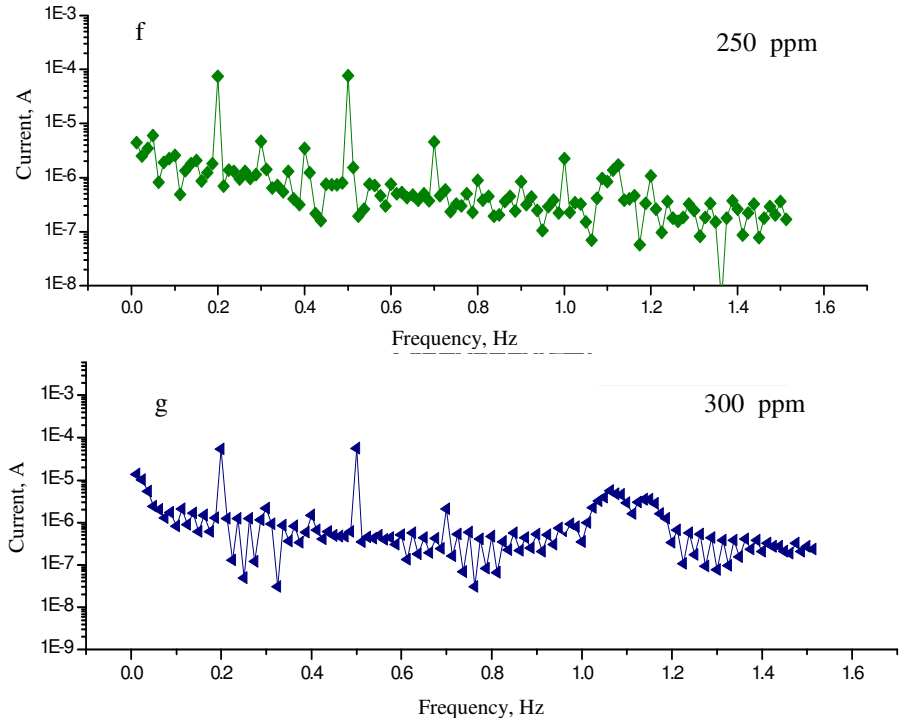

Figure 6. Intermodulation spectrum for the corrosion of MS in 1 M HCl without and with various doses of Senna extract at 25 ^{o}C

Table 4. Electrochemical kinetic parameters obtained by EFM technique for MS in 1 M HCl in the absence and presence of different doses of Senna extract at 25 ^{o}C

[inh] ppm	$i_{corr,}$ μAcm^{-2}	β_c , $mVdec^{-1}$	β_a , $mVdec^{-1}$	CF-2	CF-3	C.R , mpy	θ	%IE
0.0	1424	112	94	1.7	2.5	650.6	-	-
50	167.4	123	111	1.8	3.0	76.3	0.883	88.3
100	107.2	136	108	1.7	3.2	48.9	0.925	92.5
150	104.8	108	77	1.7	2.8	47.9	0.926	92.6
200	102.5	105	101	1.8	2.9	45.1	0.928	92.8
250	97.41	120	108	1.9	3.5	44.5	0.932	93.2
300	93.9	147	119	1.8	2.8	42.5	0.935	93.5

Adsorption isotherms

Basic information on the interaction between plant extract and metal surface can be provided using the adsorption isotherms[36]. Hence in order to gain more information about the mode of adsorption of Senna extract on MS surface in 1 M HCl at different temperatures. Attempts were made to fit experimental data with several adsorption isotherms like Langmuir, Temkin, Freundlich, Bockris–Swinkles and Flory-Huggins isotherms. However, the best fit was obtained with Langmuir isotherm which is in good agreement with Eq. 5[37].

$$C/\theta = 1/ K_{ads} + C \quad (5)$$

Where C is the inhibitor dose and K_{ads} is the adsorption equilibrium constant. The plot of C/θ against C yielded straight lines as shown in Figure 7. Using K_{ads} value, ($\Delta G°_{ads}$) was calculated from Eq. 6:

$$\Delta G^{\circ}_{ads} = -RT \ln 55.5\ K_{ads} \quad (6)$$

Where R is the gas constant and T is the absolute temperature. The value of 55.5 is the dose of water in solution in mol l^{-1}. To calculate heat of adsorption (ΔH°_{ads}), a plot of log K_{ads} *vs*. 1/T was done Figure 8. The slope would be equal to $\Delta H°_{ads}/R$ according to the following equation:

$$\text{Log } K_{ads} = (-\Delta H^{\circ}_{ads}/2.303RT) + \text{constant} \quad (7)$$

The entropy of adsorption (ΔS°_{ads}), can be obtained from the following equation:

$$\Delta G^{\circ}_{ads} = \Delta H^{\circ}_{ads} - T\ \Delta S^{\circ}_{ads} \quad (8)$$

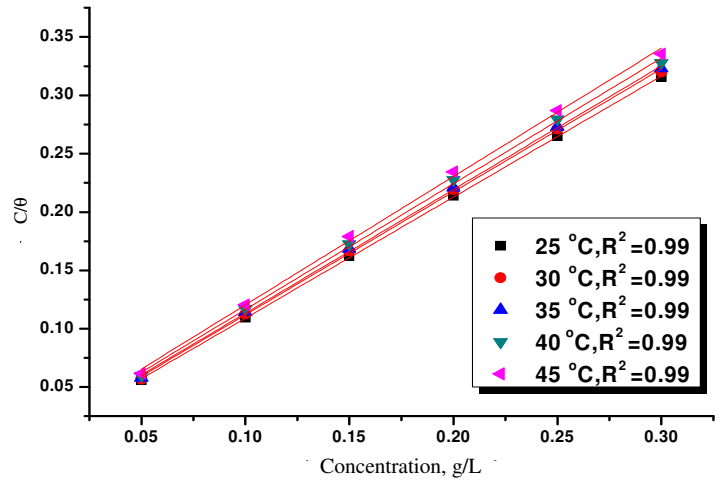

Figure 7. Langmuir adsorption plots for MS in 1 M HCl containing various doses of Senna extract at different temperatures

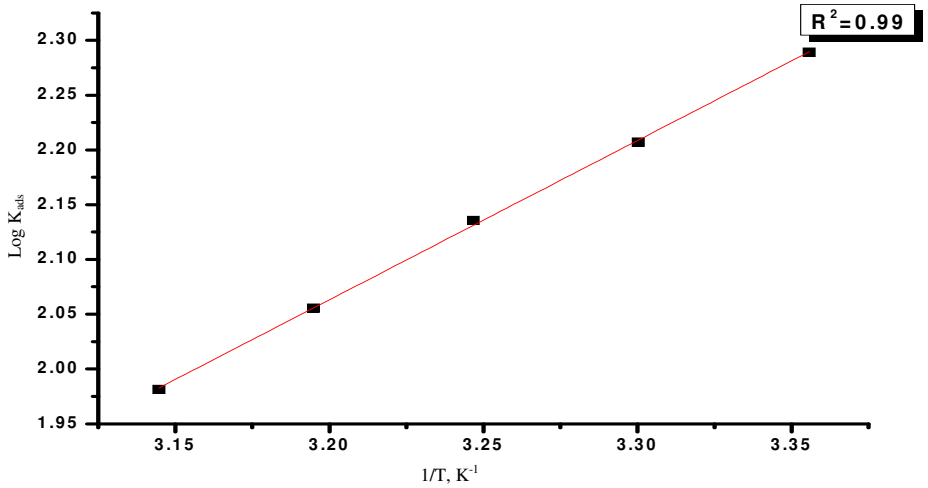

Figure 8. Log K_{ads} against 1/T for Senna extract at different temperatures (25-45 °C)

The values of K_{ads}, ΔG°_{ads}, ΔH°_{ads} and ΔS°_{ads} are listed in Table 5. The data indicate that:

i The values of K_{ads} decrease with increase in temperature. The trend observed is in agreement with Salihu *et al.,*[38] and Olasehinde *et al.*,[39] and whose reports indicated that K_{ads} obtained from the Langmuir isotherm decreased with increase in temperature.

ii The negative sign of ΔG°_{ads} indicates that the extract is spontaneously adsorbed on the metal surface[40]

iii The range of ΔG°_{ads} values around -20 kJ mol^{-1} indicating that the nature of adsorption is physical for Senna extract in 1 M HCl[41]. The negative sign of ΔH^{o}_{ads}, suggests that the adsorption of extract is an exothermic process

iv The sign of ΔS°_{ads} is negative because inhibitor molecules freely moving in the bulk solution were adsorbed in an orderly fashion on to MS resulting in a decrease in entropy[42].

Table 5. Thermodynamic parameters for the adsorption of Senna extract on MS surface in 1M HCl at different temperatures

Temperature, ^{o}C	K_{ads} M^{-1}	$-\Delta G^{o}_{ads}$, kJ mol^{-1}	$-\Delta H^{o}_{ads}$, kJ mol^{-1}	$-\Delta S^{o}_{ads}$, J $mol^{-1}K^{-1}$
25	195	23	27	77.1
30	161	22.8		75.5
35	136	22.8		74.2
40	113	22.7		72.6
45	96	22.6		71.2

Kinetic-thermodynamic corrosion parameters

The apparent activation energy E_a^*, the enthalpy of activation ΔH^* and the entropy of activation ΔS^* for the corrosion of MS samples in 1 M HCl solution in the absence and presence of different doses of Senna extract were calculated from Arrhenius and transition-state Eqs. 9 and 10.

$$\text{Rate } (k_{corr}) = A \exp(-E_a^*/RT) \quad (9)$$

$$\text{Rate } (k_{corr}) = RT/Nh \exp(\Delta S^*/R) \exp(-\Delta H^*/RT) \quad (10)$$

Where A is the Arrhenius pre-exponential factor, h is the Planck's constant and N is Avogadro's number. Figure 9 represents the plot of log k_{corr} *versus* 1/T in 1 M HCl of different doses of the extract. From the slope in Figure 9, the values of E_a^* were calculated. From Figure 10 a plot of log k_{corr} /T *versus* 1/T gives a straight line with a slope of $\Delta H/2.303R$ and intercepts of log $R/Nh + \Delta S^*/2.303$. The values of E_a^* for the inhibited solutions were greater than that of uninhibited ones indicating that the corrosion of MS was decreased due to the formation of a barrier by the adsorption of the inhibitor on the MS surface[43]. The calculated values of the (E_a^*), (ΔH^*) and the (ΔS^*) are given in Table 6. It is clear that:

i The presence of tested extract increases the E_a^* and consequently decreases the CR (k_{corr}) of MS by making a barrier to mass and charge transfer and by their adsorption on the MS surface.

ii The positive signs of ΔH^* reflect the endothermic nature of the MS dissolution process[44].

iii The values of ΔS^* in the absence and presence of tested extract are negative which indicates that the activated complex in the rate-determining step represents an association rather than dissociation[45]. This means that the activated molecules are in a higher-order state than that at the initial state.

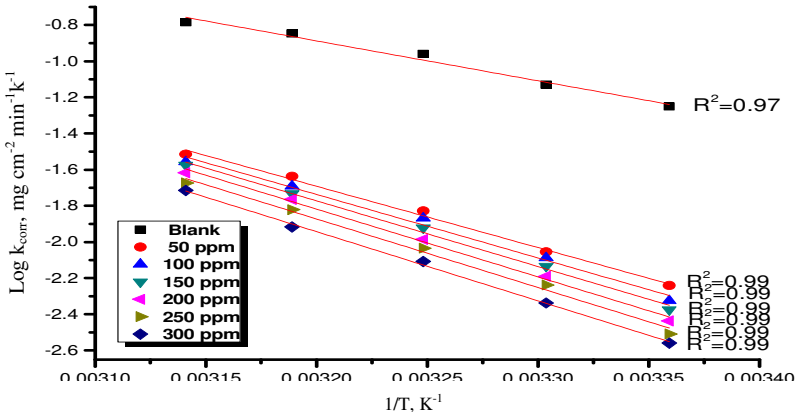

Figure 9. Arrhenius plots for MS corrosion after 120 minutes of immersion in 1 M HCl in the absence and presence of various doses of extract

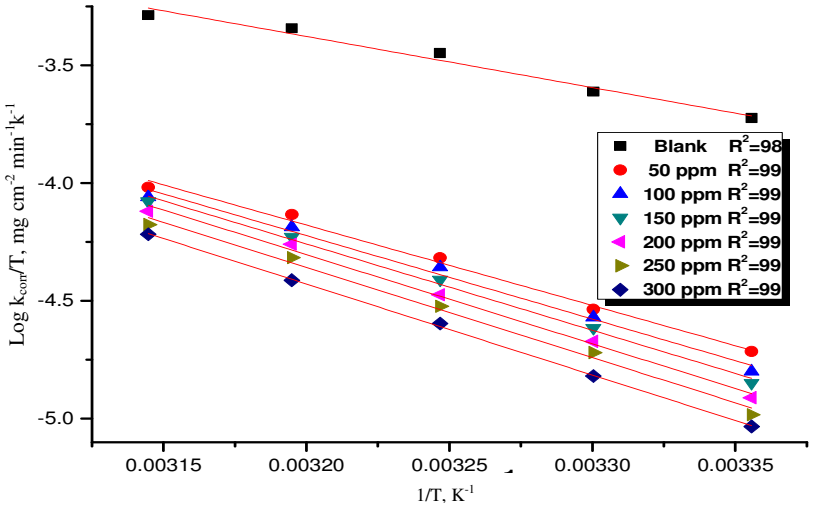

Figure 10. Transition-state for MS corrosion (log k_{corr}/T) in 1 M HCl in the absence and presence of various doses of extract

Table 6. Activation parameters for MS in absence and presence of various doses of extract in 1 M HCl

Conc. Ppm	E_a^*, kJ mol^{-1}	ΔH^*, kJ mol^{-1}	$-\Delta S^*$, J mol^{-1}K^{-1}
1 M HCl	42.2	41.5	129.1
50	64.9	65.3	68.3
100	67.2	67.7	61.5
150	69.4	70.1	54.6
200	71.7	72.4	47.9
250	72.5	73.2	46.4
300	73.2	74	45.5

Surface analysis

Scanning electron microscopy (SEM) tests

The surface morphology of MS is examined by SEM. Figure 11a-c of the MS surface in 1 M HCl solution exhibits the changes which occurred during corrosion process in absence and presence of Senna extract. Figure 11a shows SEM image of polished MS with comparatively smooth surface, MS surface after immersion in 1M HCl solution Figure 11b was drastically damaged and in presence of 300 ppm Senna extract Figure 11c surface was remarkably improved. This improvement in surface morphology indicates the formation of a protective film of Senna extract on MS surface which is responsible for inhibition and reduction in the corrosion rate[46].

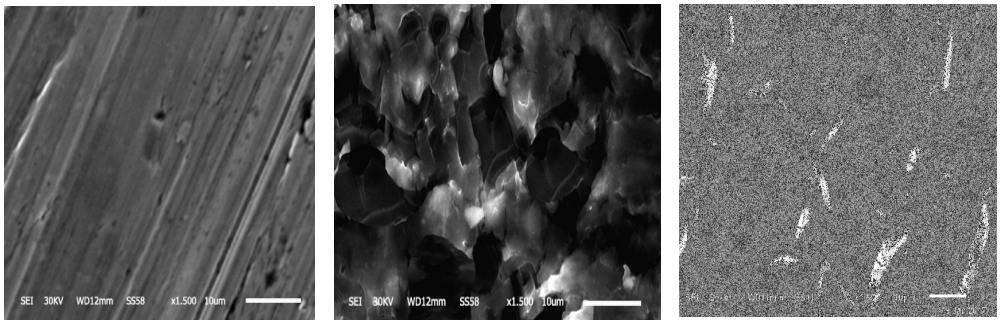

(a) (b) (c)

Figure 11. SEM micrographs of MS surface (a) before of immersion in 1 M HCl, (b) after 24 h of immersion in 1 M HCl and (c) after 24 h of immersion in 1 M HCl + 300 ppm of Senna extract at 25 ^{o}C

Atomic force microscopy (AFM) tests

Atomic force microscopy is a powerful tool to investigate the surface morphology studies which have been useful to study the influence of inhibitors on the metal/solution interface[47]. Figure 12a-c, showed the AFM 3D images of polished MS, MS in 1 M HCl without Senna extract and MS in 1 M HCl containing 300 ppm of Senna extract, respectively. As can be seen from the AFM images, the surface is very clear for polished MS specimen with average roughness 33.43 nm Figure 12a. Whereas in the absence of Senna extract, the surface of the MS is more corroded, with average roughness 667.5 nm Figure 12b. By contrast, the average roughness was reduced to 102.64 nm in the presence of Senna extract at optimum dose 300 ppm Figure 12c. From the results, we concluded that the decrease in the roughness can be very well understand to be due to the formation of adsorbed protective film of Senna extract on the MS surface.

Fourier transforms infrared spectroscopy (FT-IR) tests

FT-IR spectroscopy displays interesting features such as high signal to noise ratio, high sensitivity and selectivity, accuracy, mechanical simplicity, short analysis time and small amount of sample required for the analysis. Figure 13 shows the FT-IR spectra of the Senna extract. The broad band obtained at 3385 cm^{-1} can be assigned to (OH). The frequency at (3000 and 2916) cm^{-1}corresponds to (C-H) stretching, the one at 1635 cm^{-1} corresponds to (C=C), the -C=C stretching frequency appears at (1436 cm^{-1}) (multiple bands), the band at 1313 cm^{-1} can be assigned to (aromatic nitro compound stretching), the sharp one at 1015 cm^{-1}

corresponds to (C-O) stretch, the frequency at 952 cm^{-1} is due to (=CH_2, =C-H), the frequency at 703 cm^{-1} is due to (Nitrate NO_2 bending). By comparing the spectra of the Senna extracts with that of the solid corrosion product shown in Figure 13, it is observed that there are shifts in the frequencies. It was found that (O-H) stretch at 3385 cm^{-1} was shifted to 3361 cm^{-1}, the C=C stretch at 1635 cm^{-1} was shifted to 1631 cm^{-1}, the –C=C stretching at (1436 cm^{-1}) was shifted to 1420 cm^{-1}, the aromatic nitro compound at 1313 was shifted to 1272 cm^{-1}, (C-O) stretch at 1015 cm^{-1} was shifted to 1002 cm^{-1}, (=CH_2, =C-H) stretch at 952 cm^{-1} was shifted to 947 cm^{-1} and the Nitrate NO_2 bending frequency at 703 cm^{-1} was shifted to 740 cm^{-1}, indicating that there is interaction between the inhibitor and MS surface in the presence of 1 M HCl. The shifts in the spectra indicate that the interaction between the Senna extract and MS occurred through the functional groups presents in it. Other functional groups were missing suggesting that the adsorption of the inhibitor on the surface of MS might have occurred through the missing bonds[48]. This observation suggests that Senna extract has coordinated with Fe^{2+}, through the oxygen atom of the carboxyl group and nitrogen atom of the amine group, resulting in the formation of the Fe^{2+}- inhibitor complex on the anodic sites of the metal surface[49]. Thus, the FT-IR spectral study shows the formation of the protective film consists of Fe^{2+}- inhibitor complex.

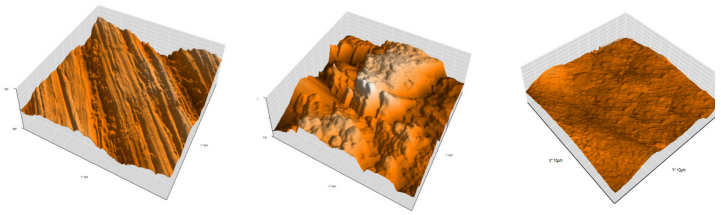

(a) (b) ©

Figure 12. AEM micrographs of MS surface (a) before of immersion in 1 M HCl, (b) after 24 h of immersion in 1 M HCl and (c) after 24 h of immersion in 1 M HCl + 300 ppm of Senna extract at 25 °C

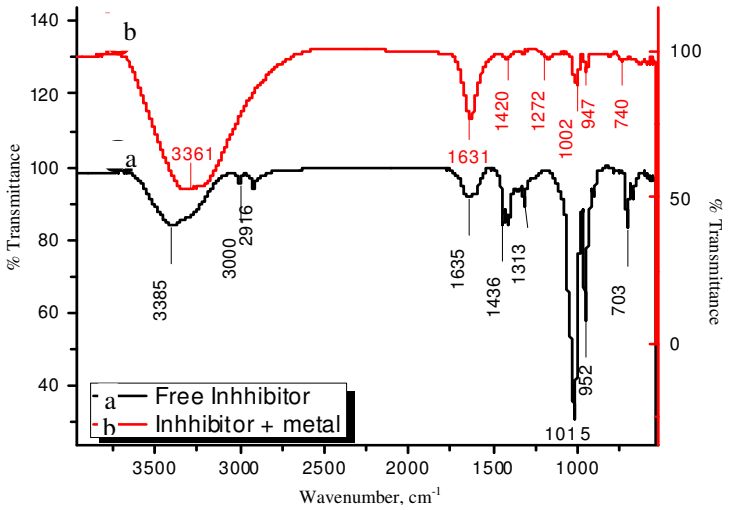

Figure 13. FT-IR spectroscopy of (a) Senna extract and (b) the film formed on the MS surface by being immersed in 1 M HCl + 300 ppm of Senna extract for 4 h at 25 °C

Mechanism of corrosion inhibition

The adsorption of extract can be described by two main types of interactions: physical and chemisorptions adsorption. In general, physical adsorption requires the presence of both the electrically charged surface of the metal and charged species in solution. The surface charge of the metal is due to the electric field existing at the metal/solution interface. A chemisorption process, on the other hand, involves charge sharing or charge transfer from the inhibitor molecules to the metal surface to form a coordinate type of a bond. This is possible in case of a positive as well as a negative charge of the surface. The presence of a transition metal, having vacant, low-energy electron orbitals (Fe^{+2} and Fe^{+3}) and an inhibitor with molecules having relatively loosely bound electrons or heteroatoms with a lone pair of electrons is necessary for the inhibiting action[50]. Generally, two types of mechanisms of inhibition were proposed. One was the formation of polymeric complexes with iron ions ($Fe^{3+)}$ depending on the applied conditions[51]. The other was the chemical adsorption of Senna extract components on iron surface[52]. The inhibition action of Senna extract does not occur by the simple blocking at the surface of iron, especially at high temperature. This might be attributed to the different adsorption capacities of the Senna extract on the MS surface at different temperatures. It has been studied that with the increase in temperature, the desorption effect of Senna extract on MS surface increased. Some of the hydrophilic groups with positively charged atoms (O^+) desorbed from the surface of MS and did more work to prevent the H^+ from getting nearer to the metal surface. Therefore, Senna extract preferentially inhibited both cathodic and anodic corrosion processes at high temperature.

Conclusion

The inhibition efficiency increases with the increase in the extract dose and decreases with the increase in temperature. Adsorption of extract molecules of the extract on MS surface is found to obey Langmuir adsorption isotherm. Polarization curves indicate that Senna extract acted as mixed type inhibitor. FT-IR spectrum revealed that the extract adsorbed on the metal surface. SEM and AFM images indicated the possibility of formation of protective film on the surface of the MS. Based on the results of WL, PP, EIS and EFM, Senna extract was shown to be an effective inhibitor for MS in 1 M HCl.

References

1. Singh D D N, Singh T B and Gaur B, *Corros Sci*., 1995, **37(6),** 1005-1019; DOI:10.1016/0010-938X(95)00010-H
2. Ashassi-Sorkhabi H, Seifzadeh D and Hosseini M G, *Corros Sci*., 2008, **50(12),** 3363-3370; DOI:10.1016/j.corsci.2008.09.022
3. Fouda A S, Eissa M, Elewady G Y, El behairy W T, Int J Electrochem Sci., 2017,**12**, 9212- 9230, DOI:10.20964/2017.10.83
4. Ali S A, Saeed M T and Rahman S U, *Corros Sci*., 2003, **45(2)**, 253-266; DOI:10.1016/S0010-938X(02)00099-9
5. Yıldırım A and Cetin M, *Corros Sci*., 2008, **50(1),** 155-165; DOI:10.1016/j.corsci.2007.06.015
6. Bartos M and Hackerman N, *J Electrochem Soc.,* 1992, **139(12),** 3428-3433; DOI:10.1149/1.2069095
7. de Souza F S and Spinelli A, *Corros Sci.,* 2009, **51(3)**, 642-649; DOI:10.1016/j.corsci.2008.12.013
8. Da Trindade L G and Goncalves R S, *Corros Sci*., 2009, **51(8),** 1578-1583; DOI:10.1016/j.corsci.2009.03.038

9. Raja P B and Sethuraman M G, *Mater Lett*., 2008, **62(17),** 2977-2979; DOI:10.1016/j.matlet.2008.01.087
10. A. Y. El-Etre, *Appl Surf Sci.,* 2006, **252(24),** 8521-8525; DOI:10.1016/j.apsusc.2005.11.066
11. Oguzie E E**,** *Corros Sci*., 2008, **50(11),** 2993-2998; DOI:10.1016/j.corsci.2008.08.004
12. Okafor P C, Ikpi M E, Uwah I E, Ebenso E E, Ekpe U J and Umoren S A, *Corros Sci.,* 2008, **50(8),** 2310-2317; DOI:10.1016/j.corsci.2008.05.009
13. Gunasekaran G and Chauhan L R, *Electrochim Acta,* 2004, **49(25**), 4387-4395; DOI:10.1016/j.electacta.2004.04.030
14. Chauhan L R and Gunasekaran G, *Corros Sci.,* 2007, **49(3),** 1143-1161; DOI:10.1016/j.corsci.2006.08.012
15. Da Rocha J C, Gomes J A D C P and D'Elia E, *Corros Sci*., 2010, **52(7),** 2341-2348; DOI:10.1016/j.corsci.2010.03.033
16. Lebrini M, Bentiss F, Vezin H and Lagrenee M, *Corros Sci*., 2006, **48(5**), 1279-1291; DOI:10.1016/j.corsci.2005.05.001
17. El-Etre A Y, *J Colloid Interface Sci*., 2007, **314(2),** 578-583; DOI:10.1016/j.jcis.2007.05.077
18. Satapathy A K, Gunasekaran G, Sahoo S C, Amit K and Rodrigues P V, *Corros Sci*., 2009, **51(12),** 2848-2856; DOI:10.1016/j.corsci.2009.08.016
19. Quraishi M A, Singh A, Singh V K, Yadav D K and Singh A K, *Mater Chem Phys*., 2010, **122(1),** 114-122; DOI:10.1016/j.matchemphys.2010.02.066
20. Rajendran S, Jeyasundari J, Usha P, Selvi J A, Regis B, Narayanasamy A P P and Rengan P, *Port Electrochim Acta,* 2009, **27(2),** 153-164; DOI:10.4152/pea.200902153
21. Khan M A, Ahmad M, Zafar M, Sultana S, Shaheen S, Leghari M K, Jan G, Ahmad F and Nazir A, *J Med Plants Res.,* 2011, **5(8),** 1471-1477.
22. Dawood K M, Shabana Y M, Fayzalla E A and El-Sherbiny E A, *J Agric Sci Mans Univ.,* 2003, **28,** 5335-5349.
23. Abd-El-Nabey B A, Abdel-Gaber A M, Ali M E S, Khamis E and El-Houssein S, *Int J Electrochem Sci*., 2013, **8**, 5851-5865
24. Vimala J R, Rose A L and Raja S, *Int J Chem Tech Res.,* 2011, **3(4**), 1791-1801.
25. Abdel- Rehim S S, Khaled K F and Abdel Shafi N S, *Electrochim Acta,* 2006, **51(16**), 3269-3277; DOI:10.1016/j.electacta.2005.09.018
26. Bosch R W, Hubrecht J, Bogaerts W F and Syrett B C, *Corrosion*, 2001, **57(1),** 60-70; DOI:10.5006/1.3290331
27. Ali S A, El-Shareef A M, Al-Ghamdi R F and Saeed M T, *Corrosion Science,* 2005, **47(11),** 2659-2678; DOI:10.1016/j.corsci.2004.11.007
28. Chakravarthy M P, Mohana K N and Kumar C P, *Int J Ind Chem.*, 2014, **5(2),** 19; DOI:10.1007/s40090-014-0019-3
29. Ferreira E S, Giacomelli C, Giacomelli F C and Spinelli A, *Mater Chem Phys.,* 2004, **83(1),** 129-134; DOI:10.1016/j.matchemphys.2003.09.020
30. Lorenz W J and Mansfeld F, *Corrosion Science,* 1981, **21(9-10**), 647-672; DOI:10.1016/0010-938X(81)90015-9
31. Rosliza R, Wan Nik W B and Senin H B, *Mater Chem Phys*., 2008, **107(2),** 281-288; DOI:10.1016/j.matchemphys.2007.07.013
32. Stoynov Z, *Electrochim Acta*, 1990, **35(10),** 1493-1499; DOI:10.1016/0013-4686(90)80003-7

33. Mansfeld F, *Electrochim Acta,* 1990, **35(10)**, 1533-1544; DOI:10.1016/0013-4686(90)80007-B
34. Bessone J, Mayer C, Jüttner K and Lorenz W J, *Electrochim Acta,* 1983, **28(2),** 171-175; DOI:10.1016/0013-4686(83)85105-6
35. Migahed M A, Zaki E G and Shaban M M, *RSC Advances,* 2016, **6(75),** 71384-71396; DOI:10.1039/C6RA12835A
36. Caigman G A, Metcalf S K and Holt E M, *J Chem Cryst*., 2000, **30,** 41-44
37. Mistry B M and Jauhari S, *Chem Engg Commun*., 2014, **201(7),** 961-981; DOI:10.1080/00986445.2013.785946
38. Ameh P O, Magaji L and Salihu T, *African J Pure Appl Chem*., 2012, **6(7),** 100-106; DOI:10.5897/AJPAC12.001
39. Olasehinde E F, Olusegun S J, Adesina A S, Omogbehin S A and Momoh-Yahayah H, *Nat Sci*., 2013, **11(1)**, 83-90.
40. Alaneme K K, Daramola Y S, Olusegun S J and Afolabi A S, *Int J Electrochem Sci*., 2015, **10,** 3553-3567.
41. Shukla S K and Quraishi M A, *Corros Sci.,* 2009, **51(9),** 1990-1997; DOI:10.1016/j.corsci.2009.05.020
42. Muthukrishnan P, Jeyaprabha B and Prakash P, *Arabian J Chem*., 2013, **10(2),** S2343-S2354; DOI:10.1016/j.arabjc.2013.08.011
43. Li X and Mu G, *Appl Surf Sci.,* 2005, **252(5),** 1254-1265; DOI:10.1016/j.apsusc.2005.02.118
44. Karthik R, Muthukrishnan P, Elangovan A, Jeyaprabha B and Prakash P, *Adv Civil Engg Mater.,* **2014**, **3(1),** 413-433; DOI:10.1520/ACEM20140010/vol.3/no.1/2014
45. Nebioglu K, Melaiye A, Hindi K M, Durmus S, Panzner M J, Hogue L A, Mallett R J, Hovis C E, Coughenour M, Crosby S D, Milsted A, Ely D L, Tessier C A, Cannon C L and Youngs W J, *J Med Chem*., 2006, **49(23),** 6811-6818; DOI:10.1021/jm060711t
46. Pitchaipillai M, Raj K, Balasubramanian J and Periakaruppan P, *Int J Minerals, Metallurgy Mater*., 2014, **21(11),** 1083-1095; DOI:10.1007/s12613-014-1013-7
47. Raja P B and Sethuraman M G, *J Mater Engg Perform*., 2010, **19(5),** 761-766; DOI:10.1007/s11665-009-9541-4
48. Wang B, Du Zhang M and Gao J, *Corros Sci*., 2011, **53**, 354-361.
49. Vera R, Schrebler R, Cury P, Del Rio R and Romero H, *J Appl Electrochem*., 2007, **37,** 519-525; DOI:10.1007/s10800-006-9284-y
50. Narvaez L, Cano E and Bastidas D M, *J Appl Electrochem*., 2005, **35(5),** 499-506; DOI:10.1007/s10800-005-0291-1
51. Li X, Deng S and Fu H, *Corros Sci.,* 2009, **51(6)**, 1344-1355; DOI:10.1016/j.corsci.2009.03.023
52. Saliyan R and Adhikari A V, *Bull Mater Sci*., 2008, **31(4),** 699-711; DOI:10.1007/s12034-008-0111-4